Idid et al., 2024
J. Basic Appl. Res biomed 10(1): 50-58

10.51152/jbarbiomed.v10i1.235

JBAAR
Journal of Basic and Applied Research in Biomedicine
ISSN 2413-7014

Original Article

Bioassay-Guided Isolation of Antimicrobial Compounds from Marine Sponge *Neopetrosia exigua*

Syed Z. Idid[1], Shahbudin Saad[2], Deny Susanti[3]

[1]Faculty of Allied Health Sciences, International Islamic University Malaysia, Kuantan, Pahang, Malaysia
[2]Department of Marine Science, Faculty of Science, International Islamic University Malaysia, Kuantan, Pahang, Malaysia
[3]Department of Chemistry, Faculty of Science, International Islamic University Malaysia, Kuantan, Pahang, Malaysia

*Corresponding Author: syedzahir@iiu.edu.my

Received: 14-10-2024
Revised: 07-11-2024
Published: 30-11-2024

Keywords:
Neopetrosia exigua, Antibacterial, Antifungi, Bisulphate avarol, Isohyrtiosine A, Demethylcystalgerone, Xestospongien

Abstract: The marine sponge *Neopetrosia exigua* has shown great potential as a source of bioactive compounds with significant antimicrobial properties. This study applied bioassay-guided fractionation to isolate and evaluate the antimicrobial activities of various compounds from *N. exigua* collected off the coast of Langkawi Island, Malaysia. Methanol extracts were partitioned into different fractions, with dichloromethane (CH_2Cl_2) and n-butanol (n-BuOH) fractions exhibiting the most potent antimicrobial activities. Four compounds were isolated: a previously undescribed bisulphate avarol derivative (**1**), two compounds isolated for the first time from *N. exigua* isohyrtiosine A (**2**) and demethylcystalgerone (**3**) and xestospongien (**4**), a known compound in *N. exigua*. The bisulphate avarol derivative (**1**) showed the most potent antibacterial effect, with the ability to inhibit *Staphylococcus aureus* at concentrations as low as 2.6 µg/mL, indicating its potential as a powerful antibacterial agent for drug development. Additionally, it exhibited strong bactericidal activity against *Bacillus cereus* and fungicidal activity against *Candida albicans* and *Cryptococcus neoformans*. Isohyrtiosine A (**2**), an indole alkaloid, exhibited moderate antimicrobial effects, while xestospongien (**4**) demonstrated broad-spectrum bacteriostatic activity. Demethylcystalgerone (**3**), a meroditerpenoid, showed selective activity against Gram-positive bacteria. These findings highlight the potential of *N. exigua* as a source of novel antimicrobial agents, particularly in combating antibiotic-resistant pathogens. Further research into the mechanisms of action and chemical diversity of sponge-derived compounds could lead to the development of new therapeutic agents for resistant infections.

Cite this article as: Idid, S.Z., Saad, S., Susanti, D. (2024) Bioassay-Guided Isolation of Antimicrobial Compounds from Marine Sponge *Neopetrosia exigua*. Journal of Basic and Applied Research in Biomedicine, 10(1): 50-58. 10.51152/jbarbiomed.v10i1.235

INTRODUCTION

The marine environment has long been recognized as a rich reservoir of bioactive compounds, offering a unique source for drug discovery, particularly in the realm of antimicrobial agents (Romano et al., 2017). Among marine organisms, sponges are prolific producers of secondary metabolites with a broad spectrum of biological activities, including antibacterial, antifungal, antiviral, and anticancer properties (Varijakzhan et al., 2021). These natural products are crucial for the survival of sponges, which are often exposed to intense competition and predation in marine ecosystems (Mehbub et al., 2024). One such sponge species, *Neopetrosia exigua*, has attracted considerable attention due to its potential in producing bioactive compounds with pharmaceutical relevance (Qaralleh, 2016).

N. exigua is a sponge species commonly found in tropical marine environments, such as the coral reefs around Southeast Asia (Majali et al., 2015). Previous research has demonstrated that marine sponges, including *N. exigua*, can yield structurally diverse compounds, many of which exhibit potent antimicrobial properties (Varijakzhan et al., 2021). These properties are especially relevant in the face of increasing antibiotic resistance among pathogens, a global challenge that demands the exploration of novel antimicrobial compounds from natural sources. In addition to its antimicrobial potential, *N. exigua* is known for producing a wide range of biologically active compounds that exhibit diverse bioactivities. Extracts and isolated compounds from *N. exigua* have demonstrated significant antimicrobial, antifungal, antiviral, cytotoxic, antitumor, antioxidant, and anti-inflammatory properties (Qaralleh, 2016). For instance, aqueous and organic extracts have shown strong antibacterial effects against pathogens like *Bacillus cereus* and *Staphylococcus aureus*, as well as antifungal activity against *Candida albicans* and *Cryptococcus neoformans* (Majali et al., 2015). Isolated compounds such as araguspongin C have exhibited promising antifungal and antifouling properties, while compounds like exiguamine A and renieramycin have shown potent cytotoxic and antiproliferative effects against cancer cells (Esposito et al., 2022). Furthermore, sterols, quinones, and alkaloids isolated from *N. exigua* continue to be investigated for their potential as therapeutic agents (Varijakzhan et al., 2021), underscoring the importance of this sponge in drug discovery research.

Antibiotic resistance has become a pressing global health crisis, with the rise of multidrug-resistant bacteria posing serious threats to public health (Minarini et al., 2020). Pathogens such as *Staphylococcus aureus*, *Escherichia coli*, and *Pseudomonas aeruginosa* have developed resistance to many conventional antibiotics, leaving clinicians with limited treatment options (Parmanik et al., 2022). According to the World Health Organization (WHO), antimicrobial resistance is projected to cause 10 million deaths annually by 2050 if new and effective drugs are not developed (O'Neil, 2014). As a result, there is an urgent need to discover novel antimicrobial agents that can combat resistant strains and reduce the burden of infectious diseases. Marine sponges, due to their unique ecological niches and chemical defense mechanisms, represent a promising but underexplored source of such novel compounds.

The bioassay-guided fractionation technique is a proven method for isolating and identifying bioactive compounds from complex mixtures, such as marine sponge extracts. This approach allows for the stepwise separation of chemical fractions based on their biological activity, enabling the identification of specific compounds responsible for antimicrobial effects. The integration of chromatographic techniques, such as thin-layer chromatography (TLC), column chromatography, and high-performance liquid chromatography (HPLC), along with spectroscopic characterization, is vital for the isolation and structural elucidation of bioactive compounds (Weller, 2012).

In this study, a bioassay-guided fractionation approach was applied to isolate antimicrobial compounds from *Neopetrosia*

exigua collected from the waters around Langkawi Island, Malaysia. Initial screening of the methanol extract of *N. exigua* demonstrated significant antimicrobial activity, which led to further fractionation using solvents of increasing polarity (Majali et al., 2015). The most active fractions were then subjected to various chromatographic techniques to purify the compounds responsible for the observed antimicrobial effects. Through these methods, this study aimed to characterize the active compounds and evaluate their antimicrobial potency against a panel of bacterial and fungal pathogens, including multidrug-resistant strains. The findings of this study highlight the potential of *Neopetrosia exigua* as a source of novel antimicrobial agents, contributing to the ongoing efforts to address the global antibiotic resistance crisis.

MATERIALS AND METHODS

Sampling and Identification

The marine sponge *Neopetrosia exigua* was collected from Langkawi Island, Malaysia (6°12′47.01″N, 99°44′39.32″E), at a depth of 1-2 meters. Following collection, the sponge was transported to the laboratory in an ice box containing dry ice. Upon arrival, *N. exigua* was cut into small pieces, immediately frozen, and stored at -20°C until extraction. The species identification was performed by Mr. Lim Swee-Cheng from the Tropical Marine Science Institute at the National University of Singapore, using skeletal slides and dissociated spicule mounts for taxonomic confirmation.

Extraction

The frozen *Neopetrosia exigua* material was thawed, thoroughly washed, and then freeze-dried to remove excess water. The freeze-dried material was homogenized and subjected to extraction with methanol (MeOH) three times, with each extraction lasting 24 hours. The supernatants were then collected, centrifuged at 10,000×g, filtered, and pooled together. The combined MeOH extracts were concentrated by removing the solvent using a rotary evaporator. The resulting MeOH extract of *N. exigua* was stored at -20°C in a deep freezer until further use.

Liquid-liquid Fractionation

A sequential gradient partitioning was conducted using different solvents to obtain fractions of compounds distributed based on their polarity. In brief, the methanol (MeOH) extract of *N. exigua* biomass was successively partitioned with n-hexane, carbon tetrachloride (CCl_4), dichloromethane (CH_2Cl_2), n-butanol (n-BuOH), and water, following the procedure described by Riguera (1997). After the solvents were evaporated using a rotary evaporator, the crude extracts from each solvent partition were labeled and stored for subsequent use.

Bioassay Guided Isolation of the Active Antimicrobial Compounds

Chromatography

Normal-phase of column chromatography was carried out on the normal-phase silica gel 70-230 mesh while reverse phase column chromatography was performed using silica gel 100 C18 (0.015 to 0.025 mm). Size-exclusion chromatography was carried out using Sephadex LH-20 as a stationary phase and MeOH as a mobile phase. Normal-phase thin layer chromatography (TLC) analysis was done on pre-coated normal phase silica gel F_{254} plates while RP-C18 silica gel F_{254} was used for the reverse phase thin layer chromatography. Spots were visualized by UV (254 and 365 nm) or iodine vapor. High Performance Liquid Chromatography (HPLC) was applied using reverse phase column. A sample was prepared in a concentration equal to 10 mg/mL and was filtrated through Millipore filter syringe (0.45 µm). A sample of 25 µL from the filtrated sample was then automatically injected. The flow rate was adjusted to 1 mL/min and the UV detector was used at two different wavelengths (210 and 280 nm).

Desalting

The desalting process was performed for CH_2Cl_2 and *n*-BuOH fractions using Amberlite XAD-2 according to the manufacturer's instruction. Briefly, 200 g from Amberlite XAD-2 was soaked in MeOH and subsequently with water for 15 minutes each. The resin suspension was packed into the column (5 cm x 1 m) and then the water was discarded. After that, slow backward water (deionised water) flow was introduced from the bottom to the top of the column in order to rearrange the resin particles according to their sizes. When the water flow stopped, the particles were then arranged as the larger ones were precipitated first (the larger ones were placed on the bottom while the smaller ones were placed on the top). Then, the sample was uploaded to the top of the column and eluted slowly with water to remove the salts while the adsorbed organic materials were eluted using MeOH.

Bio-assay guided isolation

After separation using several mobile phase systems with normal-phase TLC, the mobile phase *n*-BuOH-acetic acid-water (12:3:5) appeared to be suitable for separation of CH_2Cl_2 and *n*-BuOH constituents. Accordingly, the TLC plates were developed for CH_2Cl_2 and *n*-BuOH fractions and the spots were visualized using short and long wave UV light. The developed TLC plates were divided according to the spots presented and applied to direct contact bio-autography technique. Since CH_2Cl_2 and *n*-BuOH fractions are similar in their active constituents, they were combined in one fraction called polar fraction.

Purification of the polar fraction was started using normal-phase column chromatography. The stationary phase (silica gel 70-230 mesh) was packed in a glass column (5 cm x 1.5 m) and eluted with *n*-BuOH-acetic acid-water (12:3:5). The eluent was collected in 5 mL class vials to yield 210 sub-fractions. Next, the chemical profile of each fraction was evaluated using thin-layer chromatography (TLC) and visualized with UV light (254 nm and 365 nm). The similar fractions were combined to give 9 sub-fractions (sub-fractions A to I). After evaporation of the solvent, sub-fractions A to I were evaluated for their antibacterial activity using disc diffusion method against *S. aureus*. Among all fractions tested, sub-fractions E, F, G, and H appeared to be active. Therefore, they were selected for more purification.

The most active sub-fractions F and G that contain similar chemical profiles were combined in one fraction called FG (1.36 g). Many attempts were performed to isolate the active compounds from FG fraction using normal-phase column chromatography. But the separation of FG fraction components using normal phase chromatography was not ideal. The purification of subfraction FG was successful using RP column chromatography. The stationary phase (RP silica gel) was packed in a glass column (2.5 cm x 1 m) and eluted with a mixture of ACN in 0.01% TFA (trifluoroacetic acid) water (1:1, 3:7, 0:1, 8:2, 7:3, 6:4, 4:8). A total of 13 sub-fractions (FG1 to FG13) were collected and their antibacterial activity against *S. aureus* was evaluated.

Further purification of FG1 (41.5 mg) was performed using RP column chromatography. The stationary phase (RP silica gel) was packed in a glass column (5 cm x 1.5 m) and eluted with a mixture of MeOH-0.01% TFA water (2:8). The eluents were collected in 2 mL sub-fractions. The chemical profile of each fraction was evaluated using RP thin-layer chromatography (RP-TLC) and visualized with UV light (254 nm and 365 nm). The similar fractions were combined to give 5 sub-fractions (FG1a to FG1e). After the evaporation of the solvent, sub-fractions FG1a to FG1e were evaluated for their antibacterial activity using disc diffusion method against *S. aureus*. Based on the TLC profile, Sub-fraction FG1c contains one single spot (R_f 0.47, MeOH-0.01% TFA water (2:8)). The purity of FG1c was evaluated using analytical HPLC (**compound 1**).

Sub-fractions FG7 and FG8 were combined in one sub-fraction. Further purification of FG78 (38.6 mg) was analyzed using semipreparative RP-HPLC. The mixture of ACN-MeOH (1:1) was used as a mobile phase and three sub-fractions (FG78a, FG78b, and FG78c) were collected. In particular, about 38 mg from FG78 was injected several times to the RP-HPLC and the eluent was collected in three fractions. First fraction (FG78a) was collected in the period of 0 to 3 min as a pure single

compound (**compound 2**); second fraction was collected in the period of 3 to 7 min (FG78b) while the third fraction (FG78c) was collected in the period of 7 to 20 min. Further purification from FG78b (6.5 mg) was performed using RP-HPLC. Increasing gradient MeOH in ACN was used as a mobile phase and the eluent was collected in 30 sec intervals to yield **compound 3** (1.7 mg).

Purification of FG9 (16.8 mg) was performed using RP-HPLC. Increasing polarity of MeOH in water containing 0.01% TFA was used and the fractions were collected at in 30 sec intervals to yield **compound 4** (2.5 mg). In order to remove any trace impurities, all isolated compounds from EF fraction were purified further using Sephadex LH-20.

Characterization of the Isolated Compounds

Spectroscopy analysis including FT-IR, MS and NMR were used to characterize the isolated compounds. Infrared (IR) spectra were recorded on FT-IR Perkin Elmer 1650 using KBr disc. ^{1}H-NMR, ^{13}C-NMR and 2D-NMR were recorded on Bruker A400 (University Technology Malaysia and University Malaysia Pahang). $CDCl_3$ or CD_3OD were used as solvents. Mass spectra were recorded on JEOL MS spectrometer (University College London, UK).

Antimicrobial Assays

Microbial Strains

Two Gram-positive strains (*Staphylococcus aureus* ATCC25923 and *Bacillus cereus* ATCC11778), two Gram-negative strains (*Pseudomonas aeruginosa* ATCC27853 and *Escherichia coli* ATCC35218), and two yeast strains (*Candida albicans* ATCC10231 and *Cryptococcus neoformans* ATCC90112) were used in this study.

Disc Diffusion Method

The antimicrobial activity of the extracts was evaluated using the disc diffusion method (Majali et al., 2015). In brief, bacterial inocula, adjusted to a concentration of 10^8 CFU/mL, were evenly spread on Mueller-Hinton Agar (MHA) plates, while yeast inocula at 10^4 CFU/mL were spread on Potato Dextrose Agar (PDA). Sterile blank discs (6 mm) impregnated with the extracts or the negative control (a methanol-deionized water solution at a 4:1 ratio) were carefully placed onto the inoculated agar. The bacterial plates were incubated at 37°C for 24 hours, while the yeast plates were kept at room temperature (18-20°C) for 24-48 hours. Each sample was tested in triplicate, and the resulting inhibition zones were measured in millimeters to determine the antimicrobial efficacy.

Minimum Inhibitroy Concentration (MIC) and Minimum Bactericidal Concentration (MBC)

Three-fold serial dilutions of the isolated compounds were prepared using a 96-well plate (Majali et al., 2015) and a stock solution dissolved in methanol-deionized water (4:1). The microbial inoculum was adjusted to 10^8 CFU/mL for bacteria and 10^4 CFU/mL for yeast, and 10 µL of the inoculum was added to each well. Controls consisting of culture treated with methanol-deionized water (4:1) and untreated culture were prepared under the same conditions. The microplates were incubated for 24 hours at 37°C for bacterial strains and at room temperature for yeast strains, using a microplate reader. Turbidity in each well was measured at 600 nm for bacteria and 490 nm for yeast strains. The turbidity value of the blank well was subtracted from the turbidity measured in each treated well at each concentration. The minimum inhibitory concentration (MIC) was determined as the lowest concentration of the fraction that inhibited visible microbial growth after 24 hours of incubation.

The minimal bactericidal concentration (MBC) was determined by transferring and spreading the treated culture broth from wells with concentrations equal to or higher than the MIC value onto agar plates. The plates were then incubated at 37°C for 24 hours for bacteria, or at room temperature for 48 hours for yeasts. The MBC was defined as the lowest concentration of the fraction required to completely eliminate the test microorganism, indicated by no visible growth on the agar plates after incubation.

Direct Contact Bio-autography

The CH_2Cl_2 and n-BuOH fractions were dissolved in methanol (1 mg/mL). Using a micropipette, 2 µL of each sample was applied to the TLC plate. The TLC plates were developed twice in a solvent system of n-BuOH-acetic acid-water (12:3:5). After development, the plates were air-dried at 40°C for 3 hours. The plates were then cut into sections based on their chemical profiles, sterilized under UV light for 15 minutes, and placed onto the surface of agar inoculated with 100 µL of *S. aureus* (10^8 CFU). The plates were incubated at 4-8°C for 30 minutes, after which the TLC pieces were carefully removed using sterile forceps. The plates were then incubated at 37°C for 24 hours. The inhibition zones produced were observed, and their sizes were characterized as follows: no inhibition zone (-), small inhibition zone (+), moderate inhibition zone (++), and large inhibition zone (+++).

RESULTS

Bio-assay guided isolation

The preliminary investigation revealed that the CH_2Cl_2 and *n*-BuOH fractions showed stronger antimicrobial activity than the other fractions (Majali et al., 2015). Thus these fractions have been selected for further investigations. After several mobile phase systems were tested with normal phase TLC, the mobile phase *n*-BuOH-acetic acid-water (12:3:5) appeared to be suitable for CH_2Cl_2 and *n*-BuOH constituents to be separated. Accordingly, the TLC plates were developed for CH_2Cl_2 and *n*-BuOH fractions and using short and long wave UV light, about 11 and 13 differently coloured spots were visualized, respectively. In order to assign the active antimicrobial compounds, direct contact bio-autography technique was applied for both CH_2Cl_2 and *n*-BuOH fractions (Figure 1, Table 1). From CH_2Cl_2 fraction, three spots showed antibacterial activity including the spots with R_f values 0.18, 0.45 and 0.48. While from *n*-BuOH fraction, five spots with R_f values of 0.18, 0.45, 0.48, 0.52 and 0.60 showed antibacterial activity. Based on the R_f values, all CH_2Cl_2 active compounds were present in *n*-BuOH fraction. Both CH_2Cl_2 and *n*-BuOH fractions contain spots with R_f of 0.18, 0.45 and 0.48. Therefore, CH_2Cl_2 and *n*-BuOH fractions were combined and the fraction called as polar fraction (12.28 g).

Table 1: TLC profile and antibacterial activity of CH_2Cl_2 and *n*-BuOH fraction using direct contact bio-autography

Spot number	CH_2Cl_2		*n*-BuOH	
	R_f	Inhibition zone	R_f	Inhibition zone
1	Original spot	-	Original spot	-
2	0.18	+	Long tail	-
3	Tail	-	0.18	+
4	0.41	-	0.23	-
5	0.45	++	0.32	-
6	0.48	++	0.40	-
7	0.55	-	0.45	++
8	0.61	-	0.48	+++
9	0.64	-	0.52	++
10	0.65	-	0.60	+
11	Long tail	-	0.66	-
12			0.76	-
13			0.79	-
14			Long tail	-

The combined polar fraction (12.28 g) was subjected to normal phase column chromatography and eluted with *n*-BuOH-acetic acid-water (12:3:5) as a mobile phase. A total of 9 sub-fractions (A to I) were collected and evaluated for their antibacterial activity against *S. aureus* (Table 2). Over all sub-fractions collected, 4 sub-fractions exhibited antibacterial activity against *S. aureus*. The most active sub-fractions (F and G) appear to contain many spots with similar R_f values. In particular, all spots in G were found in F except spots with R_f values of 0.57 and 0.83. These two sub-fractions were collected in one fraction called FG (2.2 g).

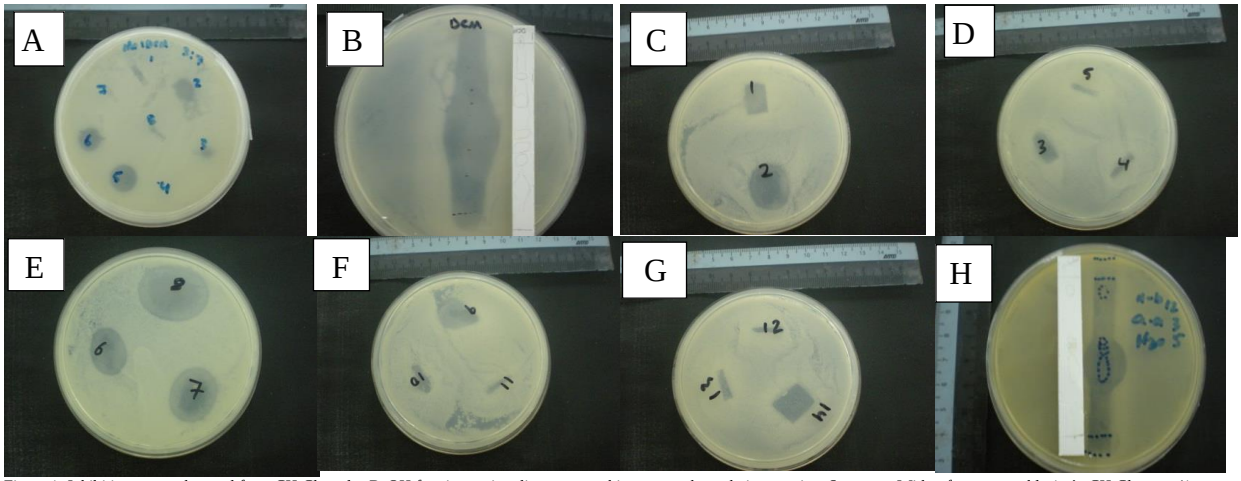

Figure 1: Inhibition zones observed from CH_2Cl_2 and *n*-BuOH fractions using direct contact bio-autography technique against *S. aureus*. With reference to table 1, A: CH_2Cl_2 spots (1 to 8), B: CH_2Cl_2 TLC plate, C: *n*-BuOH spots (1 and 2), D: *n*-BuOH spots (3, 4 and 5), E: *n*-BuOH spots (6, 7 and 8), F: *n*-BuOH spots (9, 10 and 11), G: *n*-BuOH spots (12, 13 and 14), H: *n*-BuOH TLC plate.

Table 2: TLC profile, weight and antibacterial activity of polar fraction

Sub-fractions	R_f	Weight (g)	Inhibition zone (mm)
A	0.31, 0.49, 0.52	3.010	0
B	0.31, 0.49, 0.52, 0.55, 0.7, 0.79, 0.89	2.360	0
C	0.28, 0.39, 0.46, 0.51, 0.54, 0.57, 0.61, 0.67, 0.77, 0.85	2.731	0
D	0.28, 0.39, 0.44, 0.49, 0.51, 0.54, 0.57, 0.66, 0.75, 0.87	1.276	0
E	0.25, 0.31, 0.39, 0.49, 0.57	0.733	12.3
F	0.21, 0.26, 0.31, 0.39, 0.49, 0.57, 0.83	0.816	22.0
G	0.21, 0.26, 0.31, 0.39, 0.49	0.545	24.0
H	0.21, 0.31, 0.33, 0.35	0.328	13.3
I	MeOH washing	0.154	-

Mean diameter in triplicates of zone of inhibition in mm including the diameter of the disc (6 mm). Each disc contained 100 µg extract. 0: no inhibition zone. -: not detected

RP column chromatography was used to isolate the active compounds from FG fraction (ACN and 0.01% TFA in water). A total of 13 sub-fractions (FG1 to FG13) were collected and their antibacterial activity against *S. aureus* was evaluated (Table 3).

Table 3: TLC profile, weight and antibacterial activity of FG sub-fractions

Sub-fraction	Mobile phase	R_f	Weight (mg)	Inhibition zone
FG1	Water-ACN (1:1)	0.08, 0.38, 0.52, 0.60, 0.69, 0.77, 0.88	41.5	19.3
FG2	Water-ACN (3:7)	0.54, 0.80	170.5	-
FG3	ACN	0.69, 0.39	145.8	-
FG4		0.42, 0.60, 0.71	111.6	-
FG5	ACN-MeOH(8:2)	0.44, 0.92	126.5	-
FG6		0.73, 0.34	121.4	-
FG7	ACN-MeOH (7:3)	0.44, 0.54, 0.71, 0.83	27.5	26.0
FG8		0.54, 0.67, 0.71	11.1	24.0
FG9	ACN-MeOH (6:4)	0.21, 0.38, 0.69	16.8	7.7
FG10		0.21, 0.40, 0.54, 0.65, 0.73	135.1	-
FG11		0.21, 0.40, 0.54, 0.65	120.7	-
FG12	ACN-MeOH (4:8)	0.34, 0.77	19.8	-
FG13	MeOH	0.19, 0.25, 0.46	50.3	-

Mean diameter in triplicates of zone of inhibition in mm including the diameter of the disc (6 mm). Each disc contained 100 µg extract. 0: no inhibition zone. -: not detected

The results showed that 4 sub-fractions demonstrated antibacterial activity. FG1 exhibited antibacterial activity against *S. aureus* (19 mm) as well sub-fractions FG7 (26 mm), FG8 (24 mm) and FG9 (7 mm). The fraction FG1 was subjected to the RP column chromatography (MeOH-0.01% TFA water (2:8), 2 mL). A total of 5 sub-fractions were collected and evaluated for their antibacterial activity. As shown in Table 4, all of the fractions collected exhibited antibacterial activity. The most potent sub-fraction collected was FG1c which contained only one spot with R_f value of 0.47 and its purity was confirmed using RP-HPLC (**compound 1**).

Table 4: TLC profile, weight and antibacterial activity of the compound FG1 sub-fractions

Sub-fraction	Mobile phase	R_f	Weight (mg)	Inhibition zone
FG1a	MeOH-0.01% TFA water (6:4)	0.18, 0.33, 0.42, 0.44, 0.47	11.3	7.3
FG1b		0.42, 0.44, 0.47	7.2	9.0
FG1c		0.47	3.6	27.0
FG1d		0.45, 0.47, 0.51, 0.52	9.7	15.7
FG1e		0.45, 0.47, 0.51, 0.52, 0.55, 0.57	5.3	8.7

Mean diameter in triplicates of zone of inhibition in mm including the diameter of the disc (6 mm). Each disc contained 100 µg extract.

Notably, sub-fractions FG7 and FG8 possess the most potent antibacterial compounds. The TLC analysis of these two sub-fractions revealed the presence of similar compounds including compounds with R_f values of 0.54 and 0.71. Thus, they were combined in one sub-fraction called FG78. To trace the complexity of the chemical profile of the active sub-fraction and provide guidance for further chemical isolation, FG78 was analysed using semipreparative RP-HPLC (ACN-MeOH (1:1)). Based on the HPLC profile, one single pure compound was successfully collected (compound 2, 1.9 mg) from fraction FG78a, whereas the compound collected in the period of 3 to 7 minutes (FG78b, 6.5 mg) contained some impurities. Further purification from FG78b (6.5 mg) was performed using RP-HPLC (increasing gradient MeOH in CAN, 30 sec intervals) to yield **compound 3** (1.7 mg).

Purification of fraction FG9 was performed using RP-HPLC (increasing gradient MeOH in water containing 0.01%) and the compound eluted at 3.8 minutes was collected in a single fraction and labeled as **compound 4** (2.5 mg).

Structural Charactrization of the Isolated Compounds

Compound 1

Compound **1** was obtained as pale yellow powder compound. The R_f value was determined in a mobile phase of MeOH-0.01% TFA water (6:4). The R_f value was obtained as 0.47. The CIMS spectrum (Figure S1) showed molecular ion peak at m/z 663 $[M-1]^+$, which suggested the molecular formula $C_{28}H_{41}O_{11}S_2Na_2$. The CIMS ion fragment at m/z 97 (M^++H) suggested the presence of sulfate group and ion fragment at m/z 194 (M^+-H) suggested the presence of sodium sulfate group attached to benzene ring.

The FTIR spectrum (Figure S2) showed characteristic absorption band at 1044 cm^{-1} indicated the presence of sulfate groups. Absorption bands at 2930, 3440 and 1716 cm^{-1} suggested the presence of aliphatic stretching, hydroxyl group (O-H) and carbonyl group (C=O), respectively.

The structure of compound **1** was determined through the examination of 1D and 2D NMR. ^{1}H-NMR indicated the

presence of benzene ring (Figure S3 and S4). The ^{1}H-NMR showed the presence of two ortho coupled aromatic methine protons centered at δ 7.55 (d, *J*= 8.4) and 7.15 (dd, *J*= 2.4, 8.8 Hz), and one para aromatic methine proton centered at δ 7.37 (t, *J*= 2, 4 Hz). ^{1}H-NMR also showed signals appropriate for hydroxylated drimane sesquiterpene portion to be attached to aliphatic stretching. A multiplet signal centered at δ 3.37 indicated the presence of proton at C-3. The presence of these signals suggested it to be avarol derivatives (Ovenden et al., 2011).

With the aid of DEPT experiment (Figure S5), compound **1** has 7 methine carbons, 9 methylene carbons, 5 methyl carbons and 7 quaternary carbons. The DEPT spectrum showed one quaternary carbonyl carbon signal shifted at δ 179.6 (C-15), aromatic carbon signals shifted at δ 138.6 (qC, C-20), 148.0 (qC, C-21), 124.5 (CH, C-22), 124.0 (CH, C-23), 147.1 (qC, C-24) and 119.1 (CH, C-25), and one hydroxylated carbon signal was observed at δ 77.5 (CH, C-3).

The correlation between the protons and the protonated carbons signals were assigned based on the HMQC (Figure S6). The methylene carbon shifted at δ 21.9 (CH_2, C-19) was correlated to the singlet proton shifted at δ 1.12s (H-19). The methylene carbons of hydroxylated drimane sesquiterpene portion were found to be shifted at δ 41.4 (C-1), 31.2 (C-2), 31.0 (C-6) and 29.7 (C-7) and assigned to the proton signals that shifted at δ 1.99 (overlaping, H-1), 1.43 (overlaping, H-2), 1.99 (overlaping, H-6) and 2.07 (overlaping, H-7), respectively. The olefinic methylene carbons signals shifted at δ 39.7 (C-12), 30.3 (C-13) and 29.3 (C-14) were assinged to the proton signals shifted at δ 2.07 (overlaping, H-12, H-13) and 1.43 (overlaping, H-13), respectively.

The methine carbon signals of the hydroxylated drimane sesquiterpene portion were found to be shifted δ 77.5 (C-3), 59 (C-5) and 39.9 (C-8) (Figure S7). These carbon signals showed correlation with the proton signals shifted at δ 3.37 (m, H-3), 1.43 (overlaping, H-5) and 1.99 (overlaping, H-8), respectively. Three benzene methine carbon signals shifted at δ 124.5 (C-22), 124.0 (C-23) and 119.1 (C-25) were assigned to the proton signals shifted at δ 7.55 (d, *J*= 8.4, H-24), 7.15 (dd, *J*= 2.4, 8.8, H-23) and 7.37 (t, *J*= 2.0, 4.0, H-25).

Furthermore, the HMBC spectrum (Figure S8) spectra showed that the proton signal assigned at C-19 (δ1.12) exhibited a long correlation with C-9 and C-20, which suggested this carbon to be connected between the benzene ring and the drimane sesquiterpene portion (Figure 2). The proton signal assigned at C-26 (δ 0.87) exhibited long correlation with C-9. The proton signal assigned at C-13 (δ 1.43) showed a long correlation with C-15. The assignment of all protons and carbons in this compound are summarized in Table 5.

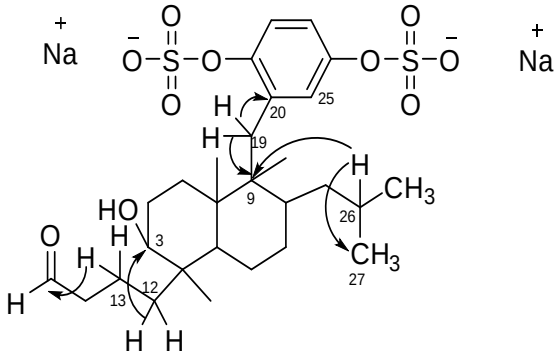

Figure 2: Long correlation of compound **1** assigned based on HMBC

Thus, the structure of compound **1** was determined to be a new derivative of avarol with two sodium sulfate groups and aliphatic side chain, which suggested the chemical structure of this compound as shown in Figure 3. The CIMS fragmentation pattern of this compound strongly supported this suggestion (Figure 4). `

Table 5: The ^{1}H and ^{13}C NMR of compound **1** (400 MHz in CDCl3)

No.	δC	DEPT	δH (*J*=Hz)	Long correlation (H to C)
1	41.4	CH_2	1.99*	
2	31.2	CH_2	1.43*	
3	77.5	CH	3.37*	
4	41.5	C	-	
5	59.4	CH	1.43*	
6	31	CH_2	1.99*	
7	29.7	CH_2	2.07*	
8	39.9	CH	1.99*	
9	45	C	-	
10	31	C	-	
11	23	CH_3	1.64*	
12	39.7	CH_2	2.07*	C-3
13	30.3	CH_2	1.43*	C-15
14	29.3	CH_2	2.07*	
15	179	C	-	
16	26	CH_2	2.28d (6.4)	
17	16	CH_3	1.34s	
18	14	CH_3	0.87*	
19	21.9	CH_2	1.12s	C-9, C-20
20	138.6	C	-	
21	148.0	C	-	
22	124.5	CH	7.55d (8.4)	
23	124.0	CH	7.15dd (2.4, 8.6)	
24	147.1	C	-	
25	119.1	CH	7.37t (2, 6)	
26	22.7	CH	0.87*	
27	38	CH_3	1.28d(12.8)	
28	34	CH_3	1.28d (12.8)	

*overlapping spectra and not clear splitting pattern

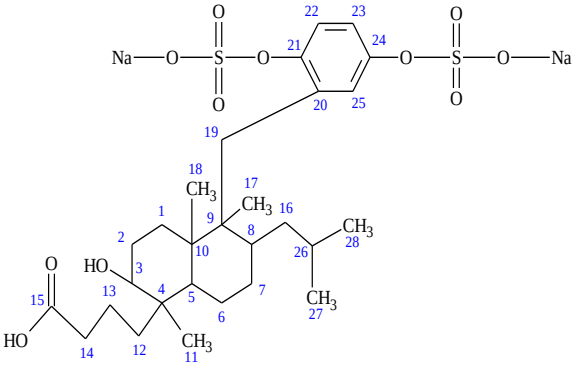

Figure 3: Chemical structure of compound **1**.

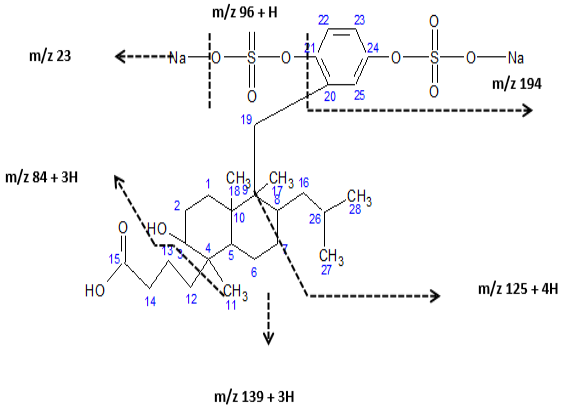

Figure 4: Mass fragmentation of compound **1**

Compound 2

Compound **2** was isolated as amorphous white powder. EIMS spectrum (Figure S9) showed pseudo-molecular ion peak at *m/z* 192 $[M^{+}-1]^{+}$ and fragment ions at 191, 160, 132, 83, 233 and 51 suggesting the molecular formula as $C_{10}H_9NO_3$.

The ^{1}H and ^{13}C-NMR signals suggested the presence of indole nucleus and one hydroxyl group (Kobayashi et al., 1990). The odd numbered molecular weight (*m/z* 191) suggested the presence of one nitrogen atom. The MS and NMR data of compound **2** suggested it to be indole derivative compound. ^{1}H-NMR (Figure S10) showed five proton signals centered at δ 7.75s (1H, H-2), 7.67s (1H, H-5), 7.22d (1H, *J*=12 Hz, H-8),

6.79dd (1H, *J*=12, 16 Hz, H-7) and 3.89s (3H, H-11). ^{13}C and DEPT spectra (Figure S11) of compound 2 showed the presence of five quaternary carbons shifted at δ 168.8, 130.0, 152.5, 127.9 and 105.8 ppm, four methine carbons shifted at δ 131.6, 104.6, 112.8 and 111.5 ppm and only one methylene carbons centered at δ 50.3 ppm. The spectroscopic data suggested **2** as indole alkaloid (Ashour et al., 2007).

The signal shifted at δ 168.8 (C-8) revealed the presence of carboxyl group while the signal shifted at δ 50.3 could be methoxy carbon. Based on the direct correlation (HMQC) and comparison with literatures, the methoxy carbon (50.3) was found to be correlated with the proton signal shifted at δ 3.89s (3H) (Figure S12). Furthur analysis from HMQC showed that the methine signals could be firmly assigned to the carbon signals shifted at δ 131.6 (C2-7.79s), 104.6 (C5-7.67), 112.8 (C7-6.79), 111.5 (C8-7.22). From EIMS spectrum, two major peaks were observed at *m/z* 160 (100) and 132 (48) which was found to be corresponded to the fragment ions generated by loss of OCH_3^+ and $OCOOCH_3$, respectively.

Based on the spectroscopic data and comparison with the literatures (Ashour et al., 2007; Youssef, 2005), compound **2** was assigned as hyrtiosine (5-hydroxy-1H-indole-3-carboxylic acid methyl ester) (Figure 5). The assignment of all protons and carbons of this compound are summarized in Table 6.

Table 6: ^{1}H and ^{13}C-NMR data of **2** (400 MHz in CD_3OD)

No.	δC	DEPT	δH (J=Hz)
NH	-	-	-
2	131.6	CH	7.79s (1H)
3	105.8	C	-
4	127.9	C	-
5	104.6	CH	7.67**
6	152.5	C	-
7	112.8	CH	6.79dd (1H, 2, 8)
8	111.5	CH	7.22d (1H, 12)
9	130.0	C	-
10	168.8	C	-
11	50.3	CH_3	3.89s (3H)

**overlapping

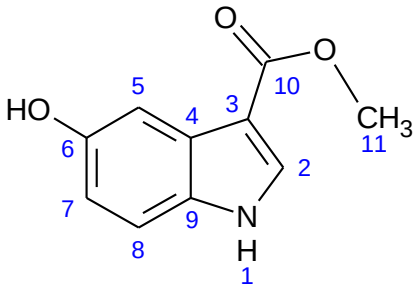

Figure 5: Chemical structure of compound **2** (5-hydroxy-1H-indole-3-carboxylic acid methyl ester)

Compound 3

Compound **3** was isolated as pale yellow powder. ESIMS spectrum (Figure S13) was showed the pseudo-molecular ion peak at *m/z* 453 $[M+Na]^+$ suggesting the molecular formula as $C_{28}H_{42}O_5$.

^{1}H-NMR spectrum (Figure S14 and S15) showed the presence of two doublet signals at δ 6.51 and 6.25 which suggested the presence of two meta coupled aromatic protons. ^{1}H-NMR also showed doublet signal shifted at δ 5.34 suggest it as an olefinic proton and an overlapping area of methylene signals shifted at δ 2.53, 3.53-3.59 and 1.5-2.37. While the proton signals of methyls were observed at δ 1.005s, 1.21-1.037m and 0.670s, one singlet signal shifted at δ 3.97, which indicated the presence of methoxy group.

^{13}C-NMR spectrum (Figure S16) showed the presence of 28 different carbon signals. The DEPT spectra showed nine quaternary carbon signals were shifted at δ 211.5, 153.1, 142.8, 136.3, 123.6, 125.4, 81.5, 55.7, and 45.5, four methine signals shifted at δ 128.6, 115.9, 112.0 and 47.1, seven methylene signals shifted at δ 47.1, 42.2, 37.9, 32.5, 29.8, 28.7 and 19.5, and seven methyl signal shifted at δ 52.3, 31.3, 26.9, 22.8, 22.0, 18.3 and 15.4. Based on the spectroscopic data, **3** was identified as meroditerpenoid with a bicyclic diterpenoid side chain. Cyclo-1`-demethylcystalgerone derivatives, which isolated from the marine algae *Cystoseira baccata*, was found to be the most analougus compound to compound **3** (Mokrini et al., 2008).

The proton and protonated carbon signals were assigned in comparsion with literature (Mokrini et al., 2008). The most shielded methyl proton signal (δ 3.97s) identified as methyoxyl proton which could be assigned to the most shielded methyl carbon shifted at δ 52.3 (C-28). However, six methyl carbon signals were existing based on the DEPT spectra, two proton singlet signals shifted at δ 1.005 and 0.670 were correlated to the carbon signal which shifted at δ 26.9 (C-16) and 22.8 (C-19), respectively. The other methyl groups must also be assigned to the singlet signal, but the methyl proton signals occure in an overlaping areas (δ 1.21 to 1.037 and 1.5 to 2.37), which indicated the presence of some impurities.

Two doublet signals at δ 6.51 (*J*= 11 Hz) and 6.25 (*J*= 10.5 Hz), which indicated the presence of two meta coupled aromatic protons have correlated with the methylene carbon signals shifted at δ 112.0 (C-23) and 115.9 (C-25), respectively. However, the doublet signal of methylene olefinic proton shifted at δ 5.34 was assigned to the methylene carbon, which shifted at δ 128.6. The quaternary carbons shifted at δ 81.5 and δ 71.1 assigned to the hydroxylated carbon (C-5 and C-15), while the quaternary signal shifted at δ 211.5 (C-12) assigned to the carbonyl group.

Based on the MS and NMR spectra, compound **3** was found to be identical to meroditerpenoids, cyclo-1`-demethylcystalgerone (Mokrini et al., 2008) (Figure 6). The assignment of all the protons and carbons in this compound are summarized in Table 7.

Table 7: ^{1}H and ^{13}C-NMR data of compound **3** (400 MHz in $CDCl_3$)

C no	δC	DEPT	δH (*J*=Hz)
1	29.8	CH_2	3.53m
2	128.6	CH	5.34d (5)
3	136.3	C	-
4	47.1	CH_2	2.53m
5	81.5	C	-
6	42.2	CH_2	2.083m
7	45.5	C	-
8	37.9	CH_2	1.62m
9	19.5	CH_2	1.67m
10	28.7	CH_2	1.92m
11	55.7	C	-
12	211.5	C	-
13	47.1	CH	3.32t
14	32.5	CH_2	1.5-2.37
15	71.1	C	-
16	26.9	CH_3	1.005s
17	31.3	CH_3	1.21-1.037
18	22.0	CH_3	1.21-1.037
19	22.8	CH_3	0.670s
20	18.3	CH_3	1.21-1.037
21	142.8	C	-
22	123.6	C	-
23	112.0	CH	6.51d (11)
24	153.1	C	-
25	115.9	CH	6.25d (10.5)
26	125.8	C	-
27	15.4	CH_3	1.5-2.37
28	52.3	CH_3	3.97s

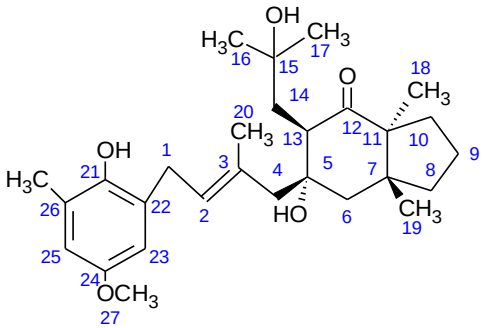

Figure 6: Chemical structure of compound **3** (cyclo-1`-demethylcystalgerone).

Compound 4

Compound **4** was isolated as amorphous white powder using reverse phase HPLC. The ESIMS spectrum (Figure S17) showed the pseudo-molecular ion peak at *m/z* 417 $[M+Na]^+$. The molecular formula was determined as $C_{14}H_{20}Br_2O_2$, since the

isotopic fragmentation pattern at m/z 415, 417 and 419, suggested the presence of two bromine atoms. Accordingly, this compound appeared to be brominated fatty acid derivatives.

^{1}H and ^{13}C-NMR spctra were used to characterize the chemical structure of **4**. The ^{1}H-NMR spectrum (Figure S18 and S19) revealed the presence of 12 different chemical shifts centered at δ 6.44, 5.84, 5.87, 4.97, 4.12, 2.54, 2.44, 2.17, 2.05, 1.56, 1.53 and 1.47. The ^{13}C-NMR and DEPT spectra (Figure S20) showed the presence of 14 carbon signals. Seven aliphatic methylene signals were found centered at δ 25.1, 27.8, 28.6, 28.8, 28.9, 35.1 and 41.6. The signals centered at δ 71.7 and 79.6 were found as oxymethines while the signal centered at δ 172.2 was found as carbonyl carbon. Four olefinic carbons were presented at δ 125.9, 1.36.5, 138.5 while the fourth carbon which was shifted at δ 88.7 was found as dibrominated olefinic carbon.

The proton and protonated carbon signals were assigned based on the HMQC spectrum (Figure S21) and comparison with the literature (Jiang et al., 2011). The methylene carbon signals shifted at δ 28.6 (C-2), 28.8 (C-3), 28.9 (C-10) and 25.1 (C-9) were found to be correlated to the proton signals shifted at the range 2.05 to 2.57. However, these proton signals were overlaped, most of the signals observed at this range exhibited multiplet splitting pattern. The methylene signals that shifted at δ 27.8 (C-11), 35.1 (C-12) and 41.6 (C-8) was assigned to the proton signals shifted at δ 1.53, 2.17 and 1.56 respectively. The oxymethine signals that shifted at δ 71.7 (C-7) and 79.6 (C-4) was assigned to the proton signals shifted at δ 4.97 and 4.12, respectively. The olefinic carbon signals that shifted at δ 125.9, 1.36.5 and 138.5 were assigned to the proton signals shifted at δ 5.77 (d, *J*=5.5 Hz), 5.84 (d, *J*= 7.6 Hz) and 6.44, respectively.

Based on spectroscopic data and comparison with the literature (Jiang et al., 2011), compound **4** was identified as xestospongien (Figure 7). The assignment of all protons and carbons in this compound are summarized in Table 8.

Table 8: ^{1}H and ^{13}C-NMR data of compound **4** (400 MHz in CDCl3)

No.	δC	DEPT	δH (*J*=Hz)
1	172.2	C	-
2	28.6	CH_2	2.05m - 2.57m
3	28.8	CH_2	2.05 - 2.44
4	79.6	CH	4.97m
5	125.9	CH	5.77d (5.5)
6	136.5	CH	5.84d (7.6)
7	71.7	CH	4.12m
8	41.6	CH_2	1.56m
9	25.1	CH_2	2.05m - 2.57m
10	28.9	CH_2	2.05 - 2.44*
11	27.8	CH_2	1.53m
12	35.1	CH_2	2.17m
13	138.5	CH	6.44t
14	88.7	C	-

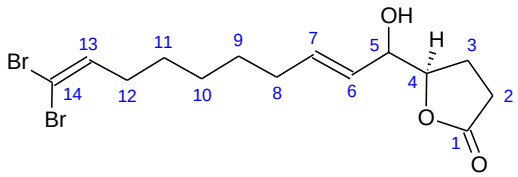

Figure 7: Chemical structure of compound **4** (Xestospongien)

Antimicrobial Activity of the isolated compounds

The antimicrobial activities of four isolated compounds from *N. exigua* were evaluated against several bacterial and fungal pathogens, including *S. aureus*, *B. cereus*, *P. aeruginosa*, *E. coli*, *C. albicans*, and *C. neoformans*. The MICs and MBCs/MFCs were determined, as shown in Table 9. Avarol (**1**) demonstrated the most potent antibacterial activity against Gram-positive bacteria, with an MIC of 2.6 µg/mL for both *S. aureus* and *B. cereus*. Its MBC values were 5.2 µg/mL and 12.6 µg/mL for *S. aureus* and *B. cereus*, respectively. Avarol (**1**) also exhibited notable antifungal activity, with MICs of 5.2 µg/mL for *C. albicans* and *C. neoformans*, and MFCs of 50 µg/mL against both fungal strains. However, its activity against Gram-negative bacteria was less pronounced, with an MIC of 17.5 µg/mL for *P. aeruginosa* and 11 µg/mL for *E. coli*, and MBC values greater than 100 µg/mL for both pathogens.

Isohyrtiosine (**2**) displayed moderate activity against Gram-positive bacteria, with MICs of 34 µg/mL for both *S. aureus* and *B. cereus*. However, its MBC values were higher than 100 µg/mL, indicating that it was less effective in killing the bacteria. Isohyrtiosine showed moderate antifungal activity, with MICs of 22 µg/mL against *C. albicans* and *C. neoformans*, but no MFCs were observed below 100 µg/mL. Notably, Isohyrtiosine was ineffective against Gram-negative bacteria, with MIC values exceeding 100 µg/mL.

Demethylcystalgerone (**3**) exhibited similar trends to Isohyrtiosine, with MICs of 11 µg/mL against *S. aureus* and *B. cereus*, but no bactericidal activity at concentrations below 100 µg/mL. The compound showed limited activity against *C. albicans* (MIC > 100 µg/mL), and it was inactive against *P. aeruginosa* and *E. coli* (MICs > 100 µg/mL).

Xestospongien (**4**) showed broad-spectrum antimicrobial activity. Against Gram-positive bacteria, it had an MIC of 11 µg/mL for both *S. aureus* and *B. cereus*, though the MBCs were greater than 100 µg/mL. Xestospongien displayed moderate activity against Gram-negative bacteria, with MIC values of 50 µg/mL for *P. aeruginosa* and 25 µg/mL for E. coli, though its MBCs were higher than 100 µg/mL. For the fungal pathogens, it had an MIC of 11 µg/mL against both *C. albicans* and *C. neoformans*, but did not display fungicidal activity at concentrations below 100 µg/mL.

Table 9: MIC, MBC and MFC (µg/mL) values of the polar isolated compounds

Microorganisms	µg/mL	Avarol (1)	Iso-hyrtiosine (2)	Demethyl-cystalgerone (3)	Xesto-spongien (4)
S. aureus	MIC	2.6	34	11	11
	MBC	5.2	>100	>100	>100
B. cereus	MIC	2.6	34	11	11
	MBC	12.6	>100	>100	>100
P. aeruginosa	MIC	17.5	>100	>100	50
	MBC	>100	-	-	>100
E. coli	MIC	11	>100	>100	25
	MBC	>100	-	-	>100
C. albicans	MIC	5.2	22	>100	11
	MFC	50	>100	-	>100
C. neoformans	MIC	5.2	22	>100	11
	MFC	50	>100	-	>100

-: Not determined.

DISCUSSION

The escalating global concern over antimicrobial resistance remains a critical issue, particularly in healthcare settings where patients are highly susceptible to infections caused by drug-resistant pathogens. These infections pose significant risks to immunocompromised individuals, such as those undergoing organ transplants, intensive care, chemotherapy, or treatment for chronic conditions like diabetes (de la Fuente-Nunez et al., 2023; Kreitmann et al., 2024). The emergence of resistant bacterial strains is driven by various factors, including the overuse and misuse of antibiotics in both clinical and agricultural contexts. As conventional antibiotics lose their efficacy, the urgent need to discover new and effective antimicrobial agents becomes more apparent (Brüssow, 2024). Marine organisms, particularly sponges, have been investigated for their unique chemical compounds, which show promise in combating resistant infections (Bharathi & Lee, 2024).

In this study, the pathogenic organisms *P. aeruginosa*, *E. coli*, *S. aureus*, and *C. albicans* were selected due to their association with various human infections. *E. coli* is known for causing a wide range of infections, including urinary tract infections, septicemia, and foodborne illnesses that can lead to severe diarrhea (Peng et al., 2024). Likewise, *S. aureus* is a leading cause of skin, bone, joint, and soft tissue infections, as well as respiratory and bloodstream infections, often complicated by methicillin-resistant *S. aureus* (MRSA) strains (Alsallameh et al., 2023).

P. aeruginosa is commonly associated with hospital-acquired infections, particularly affecting the lungs of patients with cystic fibrosis. Meanwhile, *C. albicans* frequently causes opportunistic fungal infections in immunocompromised individuals (Sathe et al., 2023). These organisms pose significant challenges in clinical settings, underscoring the urgent need for new antimicrobial agents to combat drug-resistant infections.

The antimicrobial activities of the relatively polar fractions (CH_2Cl_2 and *n*-BuOH) demonstrated greater potency compared to the *n*-hexane and water fractions (Majali et al., 2015). Notably, potent antimicrobial metabolites from sponges are typically found in these polar fractions. Marine sponges, such as *N. exigua*, face significant ecological pressures from microbial competitors, predators, and pathogens, driving them to evolve potent antimicrobial compounds as a defense mechanism (Tan, 2023).

These antimicrobial metabolites, which are often secondary metabolites, are biologically active and predominantly polar. Their polarity enables effective interaction with microbial cell membranes, disrupting essential processes like protein synthesis and membrane integrity. Additionally, the polarity of these compounds enhances their solubility in the aqueous environments where sponges reside. This increased solubility makes the metabolites more bioavailable and better suited for interacting with microbial threats. Consequently, these polar antimicrobial compounds serve as effective defense mechanisms, aiding sponges in surviving competitive, pathogen-rich habitats (Varijakzhan et al., 2021).

The highly polar fraction yielded four potent antimicrobial compounds. All the isolated compounds had been reported previously, except for the bisulphate avarol derivative. Bisulphate avarol (**1**) exhibited notable antimicrobial activity, demonstrating a bactericidal effect against Gram-positive *S. aureus* (MBC = 5.2 µg/mL) and *B. cereus* (MBC = 12.6 µg/mL). It also showed fungicidal activity against *C. albicans* (MFC = 5.2 µg/mL) and *C. neoformans* (MFC = 5.2 µg/mL). In contrast, against Gram-negative bacteria, it exhibited bacteriostatic activity, with MIC values of 11 µg/mL for *P. aeruginosa* and 17.5 µg/mL for *E. coli*. Bisulphate avarol analogues, including avarol, avaron, and bis(sulfato)-cyclosiphonodictyol, have previously been isolated from *Dysidea avara* and are known for their potent bioactivities, such as antibacterial, antifungal, antiviral, antitumor, and anti-inflammatory effects (Anjum et al., 2016; Fathallah et al., 2023; Steenblock et al., 2024).

In this study, 5-hydroxy-1H-indole-3-carboxylic acid methyl ester, an indole alkaloid derivative known as isohyrtiosine A (**2**), was isolated from the polar fraction of *N. exigua*. This compound exhibited potent bacteriostatic activity against Gram-positive bacteria (*S. aureus* and *B. cereus*) and the yeast strains tested (*C. albicans* and *C. neoformans*). Although this compound was previously reported from the marine sponge *Hyrtios erectus* (Ashour et al., 2007), this is the first report of its antimicrobial activity. Ashour (2007) also demonstrated that isohyrtiosine A exhibited cytotoxic activity at a low concentration (10.0 µg/mL). Numerous indole alkaloids isolated from marine sponges, such as cribrostatine, deoxytopsentin, and hamacanthin, have shown potent antimicrobial activity (Holland & Carroll, 2023).

The active fraction of *N. exigua* yielded a meroditerpenoid derivative with high selectivity for Gram-positive bacteria. The chemical structure of this compound was identified as cyclo-1'-demethylcystalgerone (**3**), previously isolated from the brown alga *Cystoseira baccata* (Mokrini et al., 2008). Mokrini et al. (2008) reported that cyclo-1'-demethylcystalgerone exhibited no antimicrobial activity against marine pathogenic microbes (*Pseudoalteromonas elyakovii*, *Vibrio aestuarianus*, and *Polaribacter irgensii*) or terrestrial bacteria (*Salmonella typhimurium*, *E. coli*, and *B. subtilis*). The presence of this compound in *N. exigua* suggests that it may originate from the sponge itself, its microbial symbionts, or potentially from algae or other organisms in the surrounding water (Busch et al., 2024).

Another active polar compound isolated from *N. exigua* was xestospongien (**4**), a brominated polyunsaturated fatty acid. Xestospongien exhibited bacteriostatic effects against all tested microbes. This type of metabolite is widely distributed among marine algae, sponges, tunicates, anemones, and lichens. Jiang et al. (2011) reported 39 brominated xestospongien compounds from the sponge *Xestospongia testudinaria* (Jiang et al., 2011). Xestospongien compounds have also been identified as significant antifungal and antibacterial agents (Khodzori et al., 2023).

Conclusion

This study highlights the promising antimicrobial properties of compounds isolated from *N. exigua*, including the newly identified bisulphate avarol derivative, which exhibited potent bactericidal and fungicidal activities. The presence of known compounds such as isohyrtiosine A and xestospongien underscores the chemical richness of marine sponges and their potential as sources of new antimicrobial agents. Given the global threat of drug-resistant pathogens, marine sponge-derived compounds represent a promising and largely untapped resource for the development of new antibiotics and antifungal agents. Future research should focus on exploring the full chemical diversity of marine sponges to not only identify novel compounds but also elucidate their mechanisms of action against drug-resistant microbes.

Funding Sources

This study was not supported by any sponsor or funder.

Data Availability

The original contributions presented in the study are included in the article/Supplementary material, further inquiries can be directed to the corresponding authors.

Conflict of Interest Statement

The authors have no conflicts of interest to declare.

REFERENCES

Alsallameh, S. M. S., Alhameedawi, A. K., Abbas, H. M., Khalid, D., and Kadhim, S. A. (2023). A review on methicillin-resistant Staphylococcus aureus: public health risk factors, prevention, and treatment. *Egyptian Pharmaceutical Journal*, **22**(2), 177–187. https://doi.org/10.4103/epj.epj_179_22

Anjum, K., Abbas, S. Q., Shah, S. A. A., Akhter, N., Batool, S., and ul Hassan, S. S. (2016). Marine sponges as a drug treasure. *Biomolecules & Therapeutics*, **24**(4), 347–362. https://doi.org/10.4062/biomolther.2016.067

Ashour, M. A., Elkhayat, E. S., Ebel, R., Edrada, R., and Proksch, P. (2007). Indole alkaloid from the Red Sea sponge Hyrtios erectus. *Arkivoc*, **15**, 225–231.

Bharathi, D., and Lee, J. (2024). Recent Advances in Marine-Derived Compounds as Potent Antibacterial and Antifungal Agents: A Comprehensive Review. *Marine Drugs*, **22**(8), 348. https://doi.org/10.3390/md22080348

Brüssow, H. (2024). The antibiotic resistance crisis and the development of new antibiotics. *Microbial Biotechnology*, **17**(7), e14510. https://doi.org/10.1111/1751-7915.14510

Busch, K., Marulanda-GóMez, A., Morganti, T. M., Bayer, K., and Pita, L. (2024). Sponge symbiosis: microbes make an essential part of what it means to be a sponge. In *Frontiers in Invertebrate Physiology: A Collection of Reviews* (pp. 129–195). Apple Academic Press. https://doi.org/10.1201/9781003403319

de la Fuente-Nunez, C., Cesaro, A., and Hancock, R. E. W. (2023). Antibiotic failure: Beyond antimicrobial resistance. *Drug Resistance Updates*, 101012. https://doi.org/10.1016/j.drup.2023.101012

Esposito, R., Federico, S., Bertolino, M., Zupo, V., and Costantini, M. (2022). Marine Demospongiae: A challenging treasure of bioactive compounds. *Marine Drugs*, **20**(4), 244. https://doi.org/10.3390/md20040244

Fathallah, N., Tamer, A., Ibrahim, R., Kamal, M., and Kes, M. El. (2023). The marine sponge genus Dysidea sp: the biological and chemical aspects—a review. *Future Journal of Pharmaceutical Sciences*, **9**(1), 98. https://doi.org/10.1186/s43094-023-00550-9

Holland, D. C., and Carroll, A. R. (2023). Marine indole alkaloid diversity and bioactivity. What do we know and what are we missing? *Natural Product Reports*, **40**(10), 1595–1607. https://doi.org/10.1039/D2NP00085G

Jiang, W., Liu, D., Deng, Z., de Voogd, N. J., Proksch, P., and Lin, W. (2011). Brominated polyunsaturated lipids and their stereochemistry from the Chinese marine sponge Xestospongia testudinaria. *Tetrahedron*, **67**(1), 58–68.

https://doi.org/10.1016/j.tet.2010.11.045

Khodzori, F. A., Mazlan, N. B., Chong, W. S., Ong, K. H., Palaniveloo, K., and Shah, M. D. (2023). Metabolites and Bioactivity of the Marine Xestospongia Sponges (Porifera, Demospongiae, Haplosclerida) of Southeast Asian Waters. *Biomolecules*, **13**(3), 484. https://doi.org/10.3390/biom13030484

Kobayashi, J., Murayama, T., Ishibashi, M., Kosuge, S., Takamatsu, M., Ohizumi, Y., Kobayashi, H., Ohta, T., Nozoe, S., and Takuma, S. (1990). Hyrtiosins A and B, new indole alkaloids from the Okinawan marine sponge Hyrtios erecta. *Tetrahedron*, **46**(23), 7699–7702. https://doi.org/10.1016/S0040-4020(01)90065-1

Kreitmann, L., Helms, J., Martin-Loeches, I., Salluh, J., Poulakou, G., Pène, F., and Nseir, S. (2024). ICU-acquired infections in immunocompromised patients. *Intensive Care Medicine*, **50**(3), 332–349. https://doi.org/10.1007/s00134-023-07295-2

Majali, I., Qaralleh, H. N., Idid, S. Z., Saad, S., Susanti, D., and Althunibat, O. Y. (2015). Potential antimicrobial activity of marine sponge neopetrosia exigua. *Journal of Basic and Applied Research*, **1**(1), 1–13.

Mehbub, M. F., Yang, Q., Cheng, Y., Franco, C. M. M., and Zhang, W. (2024). Marine sponge-derived natural products: trends and opportunities for the decade of 2011-2020. *Frontiers in Marine Science*, **11**, 1462825. https://doi.org/10.3389/fmars.2024.1462825

Minarini, L. A. D. R., Andrade, L. N. de, De Gregorio, E., Grosso, F., Naas, T., Zarrilli, R., and Camargo, I. L. B. C. (2020). antimicrobial resistance as a global public health problem: how can we address it? In *Frontiers in Public Health* (Vol. 8, p. 612844). Frontiers Media SA. https://doi.org/10.3389/978-2-88966-284-5

Mokrini, R., Mesaoud, M. Ben, Daoudi, M., Hellio, C., Maréchal, J.-P., El Hattab, M., Ortalo-Magné, A., Piovetti, L., and Culioli, G. (2008). Meroditerpenoids and derivatives from the brown alga Cystoseira baccata and their antifouling properties. *Journal of Natural Products*, **71**(11), 1806–1811. https://doi.org/10.1021/np8004216

O'Neil, Jjart. (2014). Antimicrobial resistance: tackling a crisis for the health and wealth of nations. In *London: Review on Antimicrobial Resistance*. https://wellcomecollection.org/works/rdpck35v

Ovenden, S. P. B., Nielson, J. L., Liptrot, C. H., Willis, R. H., Tapiolas, D. M., Wright, A. D., and Motti, C. A. (2011). Sesquiterpene benzoxazoles and sesquiterpene quinones from the marine sponge Dactylospongia elegans. *Journal of Natural Products*, **74**(1), 65–68. https://doi.org/10.1021/np100669p

Parmanik, A., Das, S., Kar, B., Bose, A., Dwivedi, G. R., and Pandey, M. M. (2022). Current treatment strategies against multidrug-resistant bacteria: a review. *Current Microbiology*, **79**(12), 388. https://doi.org/10.1007/s00284-022-03061-7

Peng, Z., Wang, X., Huang, J., and Li, B. (2024). Pathogenic Escherichia coli. In *Molecular Medical Microbiology* (pp. 1065–1096). Elsevier. https://doi.org/10.1016/B978-0-12-818619-0.00069-1

Qaralleh, H. (2016). Chemical and bioactive diversities of marine sponge Neopetrosia. *Bangladesh Journal of Pharmacology*, **11**(2), 433–452. https://doi.org/10.3329/bjp.v11i2.26611

Romano, G., Costantini, M., Sansone, C., Lauritano, C., Ruocco, N., and Ianora, A. (2017). Marine microorganisms as a promising and sustainable source of bioactive molecules. *Marine Environmental Research*, **128**, 58–69. https://doi.org/10.1016/j.marenvres.2016.05.002

Sathe, N., Beech, P., Croft, L., Suphioglu, C., Kapat, A., and Athan, E. (2023). Pseudomonas aeruginosa: Infections and novel approaches to treatment Knowing the enemy the threat of Pseudomonas aeruginosa and exploring novel approaches to treatment. *Infectious Medicine*, **2**(3), 178–194. https://doi.org/10.1016/j.imj.2023.05.003

Steenblock, C., Richter, S., Lindemann, D., Ehrlich, H., Bornstein, S. R., and Bechmann, N. (2024). Marine Sponge-Derived Secondary Metabolites Modulate SARS-CoV-2 Entry Mechanisms. *Hormone and Metabolic Research*, **56**(4), 308–317. https://doi.org/10.1055/a-2173-0277

Tan, L. T. (2023). Impact of marine chemical ecology research on the discovery and development of new pharmaceuticals. *Marine Drugs*, **21**(3), 174. https://doi.org/10.3390/md21030174

Varijakzhan, D., Loh, J.-Y., Yap, W.-S., Yusoff, K., Seboussi, R., Lim, S.-H. E., Lai, K.-S., and Chong, C.-M. (2021). Bioactive compounds from marine sponges: Fundamentals and applications. *Marine Drugs*, **19**(5), 246. https://doi.org/10.3390/md19050246

Weller, M. G. (2012). A unifying review of bioassay-guided fractionation, effect-directed analysis and related techniques. *Sensors*, **12**(7), 9181–9209. https://doi.org/10.3390/s120709181

Youssef, D. T. A. (2005). Hyrtioerectines A− C, Cytotoxic Alkaloids from the Red Sea Sponge Hyrtios e rectus. *Journal of Natural Products*, **68**(9), 1416–1419. https://doi.org/10.1021/np050142c